Assessment protocols and comparison of ordering relations for spectral image processing

Hilda Deborah, Noël Richard, Jon Yngve Hardeberg, and Christine Fernandez-Maloigne

Abstract—Recent developments in hyperspectral sensors allow to obtain high spectral and spatial resolutions that are close to the optical and physical structures of acquired surfaces. Consequently, hyperspectral imaging is used for its potential gain of accuracy. To preserve this metrological potential, generated bias, errors, and uncertainties must be managed at all subsequent processing levels. Based on the argument that a spectral image processing should avoid the linear approach, this study proposes several protocols for assessing the quality of spectral ordering relations. The protocols include considerations of theoretical properties to ensure result stability, in physical aspects of spectral processing to ensure the link to physical properties of materials, and experimental results using spectral images with physical ground truth to assess bias and errors. Full-band ordering relations are compared in order to find which satisfies all of the expected properties of a metrological spectral image processing.

Index Terms—Multidimensional signal processing, image processing, imaging spectroscopy, metrology

I. INTRODUCTION

In digital image processing, linear approaches have been extensively used in variety of applications, mainly for their simple mathematical expressions and technical implementations. However, it has to be noted that linear processing techniques require valid addition and multiplication with a scalar. And if the prerequisites are not satisfied, it is erroneous to employ the linear approach. When it comes to the spectral domain, no valid addition and multiplication with a scalar are defined for it. This means that the linear approach should be avoided. Additionally, its use is not recommended since it demonstrates inability to deal with nonlinearities, e.g., impulse noise, non-linear image degradations, etc.

Limitations of the linear approach to image processing can be overcome by the nonlinear ones, e.g., mathematical morphology (MM), rank order filters (ROF), nonlinear image restoration, etc. Many of these techniques, e.g., MM and ROF, are built on the notion of ordering relation. But the use of nonlinear techniques are not without challenge. For the ordering-based ones, it is only the scalar domain that is naturally equipped with an ordering relation [1], [2]. And when it comes to the spectral domain, the challenge becomes two folds. The first is in obtaining a theoretically valid multivariate ordering relation, and the second is in obtaining one that is suitable for the spectral domain, considering all characteristics and specificities of the data. A spectral image is not a mere three-dimensional mathematical object, but a measurement obtained from a physical light sensor [3]. A recent theoretical advance concluded that a spectral pixel should be considered as a digitized continuous function of the wavelength [4]. Then,

among the existing multivariate ordering relations, which one is the most correct and suitable for use in the spectral domain?

Ordering relation in the scalar domain naturally presents a physical sense. E.g., a grayscale image can be considered as an intensity image and, thus, its pixel values correspond to the amount of energy captured by an image sensor. A spectral image can be considered as multiple intensity images, each corresponds to a specific wavelength. Therefore, a multivariate ordering relation which is partially coherent with regards to physical senses of the image can be obtained. However, there is no evident way to produce such ordering relation. Even though it is still possible, there are two constraints to be met. This ordering relation must stay close to the physical aspects of data, such that the produced results are understandable. Then, it has to respect the theoretical properties of an ordering relation, such that results are predictable regardless of the spectral content.

In order to select the most suitable ordering relation for applications in computer vision, we focus on establishing a standard protocol for the comparison of spectral ordering relations. Then, since a spectral image is a measurement, it is imperative that the protocols take also into account the metrological aspects of this data. But before going into the protocols, Section II provides the state of the art of multivariate ordering relations that have been applied or are applicable to the spectral domain. This section will also give a discussion of their suitability for use in the domain. Two protocols assessing accuracy and efficiency can be read in Section III and IV, respectively. Both protocols are built around the computation of median, which is directly attainable after defining an ordering relation. MM is a more advanced image processing framework that is based on ordering relation. But in order to obtain it for the spectral domain, there are several theoretical properties to be satisfied, and they are provided in Section V. This section provides a discussion on which ordering relation has the desired properties, which does not and what causes it. In section VI, the usefulness of an ordering relation is measured through measuring the performance of spectral Beucher's gradient. Gradient is an important operator allowing to carry out segmentation algorithm using watershed. Therefore, quality of the segmentation result highly depends on quality of the employed gradient operator. In Section VII, we provide how to combine the different assessment results to define the most suitable ordering relation for spectral image processing, embedding metrological constraints. Finally, the article is concluded in Section VIII. Mathematical notations frequently used throughout the article can be found in Table I.

II. Spectral ordering relations

An early study of multivariate ordering relation classified the existing approaches into four non-mutually exclusive groups, i.e., marginal, partial, conditional, and reduced approaches [5]. Since then, multitudes of multivariate ordering relations have been developed. A more recent state of the art study is available, providing a discussion based on the theoretical properties of an ordering relation, i.e., pre-, partial, and total-orders [6]. In the following, the state of the art is narrowed down to the spectral ones, including color and general multivariate ordering relations that are directly extensible to the spectral domain. Note that, unless specified, the ordering relation between two arbitrary spectral functions S_1 and S_2 using any arbitrary ordering function g provided in this section is defined as in (1).

$$S_1 \preceq_g S_2 \Leftrightarrow g(S_1) \leq g(S_2) \tag{1}$$

A. Marginal and energy-based ordering relations

Marginal ordering relation orders spectral data channel-wise, followed by strategies to combine the channel-wise results [7]. Its mathematical expression in (2) shows that the binary relation $\leq$ has to be satisfied in all spectral ranges.

$$S_1 \preceq_{\text{marg}} S_2 \Leftrightarrow s_1(\lambda) \leq s_2(\lambda), \, \forall \lambda \in [\lambda_{\min}, \lambda_{\max}] \tag{2}$$

However, a spectral function or, simply, a spectrum is not always larger than another in all wavelengths, making expression (2) fail to give a decision. A commonly employed strategy to address this problem is illustrated by the minimum extraction in (3). Given a set of spectra to order $\mathscr{S}$, its minimum spectrum is one whose value is minimum in all wavelengths, thus creating a new spectrum that does not exist in the initial spectral set. This introduction of a new data is called *false spectra* problem, see Section V-B. Another drawback of the marginal approach is its inability to exploit inter-channel correlations in a hyperspectral image. Further on, this ordering relation will be referred to as **Marg**.

$$g_{\text{marg}}^-(\mathscr{S}) = \bigwedge_{\lambda_{\min} \leq \lambda \leq \lambda_{\max}} \{s_i(\lambda)\}, \, \forall S_i \in \mathscr{S} \tag{3}$$

Images in the grayscale domain can be considered as intensity images. Considering a spectrum as energy, one is larger than another when it has a bigger sum of energy (4). Thus, as in the grayscale domain, a 'white' spectrum is always larger than a 'black' one [8]. This ordering relation will be referred to as **Esum**.

$$g_{\text{esum}}(S) = \int s(\lambda) d\lambda \tag{4}$$

B. Ordering relations with a prioritization function

Given a certain condition, a lexicographic approach sequentially orders spectra by means of their marginal components. If its original mathematical expression in (5) is to be considered as is [6], a spectrum would be expressed as a set of values obtained from n discrete spectral bands, i.e., $S_1 = \{s_1(\lambda_i)\}$, for $\lambda_{\min} = \lambda_1 \leq \cdots \leq \lambda_i \leq \cdots \leq \lambda_n = \lambda_{\max}$. This ordering relation can be a good choice when priorities among image channels

S	A spectral function or spectrum expressed as a continuous function of wavelength, $S = \{s(\lambda)\}$
$I(x)$	Image or pixel value associated with spatial coordinate x; the pixel of a spectral image is defined as $I(x) = S$
λ	Wavelength or spectral band/ channel, $\lambda \in [\lambda_{\min}, \lambda_{\max}]$
$g(S)$	Ordering function applied on spectrum S
$a \Leftrightarrow b$	Logical ordering relation a is equal by definition to logical ordering relation b
$S_1 \preceq_g S_2$	Logical ordering relation "less than or equal to" between arbitrary spectra S_1 and S_2, with respect to any arbitrary ordering relation g
$\prec_g, \succ_g, =_g$	Logical ordering relations "less than", "greater than", and "equal to" relative to any arbitrary g, respectively
$S_1 = S_2$	Any arbitrary spectra S_1 and S_2 have equal values in all wavelengths, $\{s_1(\lambda) = s_2(\lambda), \forall \lambda \in [\lambda_{\min}, \lambda_{\max}]\}$
$d(S_1, S_2)$	Distance between two arbitrary spectra S_1 and S_2, also used in the context of line profile using distance function
S_{ref}	Spectral reference in distance-based ordering relations
$S^{-\infty}, S^{+\infty}$	Spectral references associated to minimum and maximum rank extraction in an ordering relation, respectively
$\mathscr{S}$	A set of spectral functions
W	Filter window defining a neighborhood over the spatial dimension of an image. Also used to denote structuring element in the context of mathematical morphology
L	A line segment over the spatial dimension of an image
$\mathscr{S}_W(x),$ $\mathscr{S}_L(x)$	Spectral set $\mathscr{S}$ within filter window W or line segment L as a function of spatial coordinate x
r	Rank or order
$F_{W,r,g}(x)$	Spectral filter replacing the spectral function at x with one having rank r relative to ordering function g in the neighborhood W
$\#\mathscr{S}$	Cardinality of the set $\mathscr{S}$
ℓ	Line profile
S_{wh}	Theoretical equi-energetic white spectrum
$\delta, \varepsilon, \varphi$	Morphological dilation, erosion, and gradient, respectively
μ, σ	Mean and standard deviation, respectively
$\wedge, \vee$	Point-wise minimum and maximum, respectively, in discrete intervals or, in the continuous case, *infimum* and *supremum*, respectively

are known. Otherwise, only the first few channels will be considered while the rest rendered almost negligible. To the best of our knowledge, this construction has mostly been used in the color domain [9]. In the spectral domain, lexicographical cascade is used to resolve classification ties in supervised ordering [10] or to allow reaching the total ordering property [8], [11]. Throughout this article, this ordering relation will be referred to as **Lex**.

$$S_1 \preceq_{\text{lex}} S_2 \Leftrightarrow \exists \lambda_i \in [\lambda_1, \lambda_n],$$
$$(\forall \lambda_j < \lambda_i, s_1(\lambda_j) = s_2(\lambda_j)) \text{ AND } (s_1(\lambda_i) \leq s_2(\lambda_i)) \tag{5}$$

Nevertheless, adapting (5) to a continuous form, it can be generalized into a prioritization function of the image channels as in (6). In this expression, any arbitrary prioritization function $f(\lambda)$ can be used.

$$g_{\text{P}}(S) = \int_{\lambda_{\min}}^{\lambda_{\max}} f(\lambda) \cdot s(\lambda) \, d\lambda \tag{6}$$

In [12], two kinds of prioritization are used to give priority to the shorter or longer wavelengths according to the color content, i.e., more bluish or reddish. Using a center wavelength is possible using a modulo$_{[\lambda_{min}\lambda_{\max}]}$ representation but the physical sense of the data will be lost since wavelengths closer

to the center wavelength at the left will have a very different priority than those at the right.

Bit mixing approach [13] can also be rewritten as prioritization function-based ordering relation. However, its prioritization function is applied not only on the spectral channels but also at the data bits. It considers each spectral value $s(\lambda)$ as a binary word consisting of B bits, within a sequence of words, one per channel, i.e. $s(l)_{\{b\}}$, $b \in [0, B-1], l \in [0, N-1]$ with N the channel count. The complete sequence constructs a word of $B \times N$ bits, see (7). A priority can then be defined for the shorter or longer wavelengths through the function $k(l)$.

$$g_{\text{BM}}(S) = \sum_{b=0}^{B-1} \left(2^{B \cdot b} \sum_{l=0}^{N-1} k(l) \cdot s(l)_b \right), \text{ where}$$
$$k(l) = \begin{cases} 2^{N-l} & \text{Priority for the shorter wavelengths} \\ 2^l & \text{Priority for the longer wavelengths} \end{cases} \quad (7)$$

C. Distance-based ordering relations

By defining a distance function and a spectral reference, ordering relation in (8) is obtained. It has been employed in [14]. If the selected reference is a theoretical equi-energetic white spectrum, g_{d1} will behave similarly to g_{Esum} [8].

$$g_{d1}(S) = d(S, S_{\text{ref}}) \quad (8)$$

Aiming to fully control the convergence of image value set in a morphological context, Convergent Color Mathematical Morphology (CCMM) [15] employs two spectral references separately for minimum and maximum extraction, g_{CCMM}^{-} and g_{CCMM}^{+} respectively. CCMM, as expressed in (9), is directly extensible to the hyperspectral domain. However, it is not idempotent and, thus, not a suitable choice for constructing an MM framework for spectral data.

$$g_{\text{CCMM}}^{-}(S) = d(S, S^{-\infty}) \text{ and } g_{\text{CCMM}}^{+}(S) = d(S, S^{+\infty}) \quad (9)$$

Cumulative distance based ordering relation in (10) has been employed in a median filtering [16] and for an extension of MM to the hyperspectral domain [17]. In later sections, when this ordering relation is used, it will be referred to as **Cumdist**. Throughout this article, Cumdist embeds KLPD function [4] as its spectral difference function d.

$$g_{dn}(S) = \sum d(S, S_i), \forall S_i \in \mathscr{S}_W \quad (10)$$

D. Supervised ordering approaches

Assuming background-foreground representations in an image, kriging interpolation and SVM were employed to learn an ordering relation [11]. When both representation sets are unitary, the ordering relation is as in (11), where S_b and S_f correspond to background and foreground pixels, respectively, and K is points' pairwise covariances in kriging interpolation.

$$g_{\{S_b, S_f\}}(S) = \frac{K(S_f, S) - K(S_b, S)}{K(S, S) - K(S_f, S_b)} \quad (11)$$

The two-class construction in (11) was further developed into a multiclass one [18] in (12). g^* is a normalized two-class function, e.g., one-vs-all SVM evaluation function, $\mathscr{S}_i$ is a set

of spectral functions belonging to class i, and $\mathscr{S}_{-i}$ is a set of spectral functions belonging to classes other than i.

$$g_{\{\mathscr{S}\}}(S) = \max_i g^*(S; \mathscr{S}_{-i}, \mathscr{S}_i) \quad (12)$$

Other supervised ordering relations for hyperspectral images can be found in [19], [10], [20]. Generally, the main drawback of this approach lies in its assumption of background-foreground or multiclass representations. Indeed, the assumption can be highly relevant under the context of remote sensing images or for classification purposes, but it still renders a limited use of the approach. As an example, hyperspectral images of paintings cannot always be modeled as background-foreground representations or the multiclass one due to the mixing nature of pigments and other chemical materials. And since such approaches reduce the acquired spectral accuracy to several classes or levels, they are not suitable for metrological purposes of, typically, texture analysis.

E. Ordering relations with prior data reduction

Computational cost is often an important consideration for hyperspectral image processing. The large channel count of a hyperspectral image poses challenges in memory size and also computational time and complexity. To deal with the issue, dimensionality reduction [21], [22] or band selection [23] are often employed as a preprocessing step. It is then followed by any ordering relations mentioned previously. Despite the high interest of such approaches, this study will not consider them. This is because with the reduction steps, it is difficult to distinguish the impact of only the ordering relation. And, eventually, the final processing results should be considered as the product of both reduction process and ordering relation.

F. A full-band and metrological spectral ordering relation

In [12], an ordering relation based on the ratio of distance relative to two spectral references was proposed, referred to as **CRA**. It is a conditional ordering relation where the first and second conditions are ratio of distance proportional to magnitude and shape differences between two spectra, respectively. Its mathematical construction can be seen in (13). CRA employs two different equations for its maximum and minimum extractions, which are dual since $R_0 = (R_1)^{-1}$. It is further illustrated in Fig. 1 as a geometric distance between S_1 and S_2 in a two-dimensional coordinate system with $S^{-\infty}$ and $S^{+\infty}$ as the origins. The selection of $S^{-\infty}$ and $S^{+\infty}$ can be arbitrarily or according to specific application goals. A guidance in selecting the optimum pair of references can be found in [12]. This ordering relation was developed to extend MM framework to the spectral domain, aiming to respect both of its theoretical and metrological constraints.

$$S_1 \preceq_{\text{CRA}} S_2 \Leftrightarrow \begin{cases} R_0(S_1) > R_0(S_2) \text{ or} \\ R_0(S_1) = R_0(S_2) \text{ and } R_2(S_1) < R_2(S_2) \end{cases}$$
$$S_1 \succeq_{\text{CRA}} S_2 \Leftrightarrow \begin{cases} R_1(S_1) > R_1(S_2) \text{ or} \\ R_1(S_1) = R_1(S_2) \text{ and } R_2(S_1) > R_2(S_2) \end{cases} \quad (13)$$
$$R_0 = \frac{d(S_i, S^{+\infty})}{d(S_i, S^{-\infty})}, R_1 = \frac{d(S_i, S^{-\infty})}{d(S_i, S^{+\infty})}, R_2 = \frac{2 \cdot d(S_i, S^{-\infty})}{d(S^{-\infty}, S^{+\infty})}$$
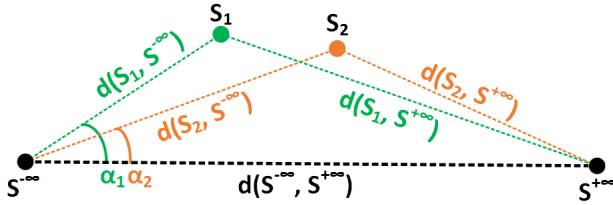
Fig. 1. Illustration of conditional ratio and angular (CRA) ordering relation in a two-dimensional space with $S^{-\infty}$ and $S^{+\infty}$ as the origins.

III. ACCURACY[1] OF SPECTRAL MEDIAN FILTERS

Maragos [25], [26] and Pitas [27] have laid down all theoretical foundations for median filters and their relationship to morphological filters and the linear filtering approaches. Demonstrations of their properties, i.e., edge detection and noise suppression, were developed for the grayscale domain without any questions regarding the ordering relation. However, to keep these properties in the multivariate case of median filters, the ordering relation must be total. Thus the relationship between the ordering relation and filtering properties is injective. In this paper, we impose an additional constraint since having a total ordering property is insufficient for the filters to be valid. The additional constraint requires the ordering to also respect the physical sense of spectral measures. But since the satisfaction of this last constraint is difficult to establish, experimental tests are required. And as a hypothesis, the ordering relation can be valid if all properties of the median filters are obtained. Thus, the assumption is based on the possible bijectivity of relationship linking the validity of ordering relation and the filtering properties. To assess the validity of the ordering relation, satisfaction of the filtering properties will be measured in the experimental tests. Edge preservation test is chosen in the following as it is based on the one developed by Pitas [27], thus ensuring a direct translation from Pitas' foundation.

This first protocol of ordering relation assesses ordering errors and biases. It proposes to compare the median extracted through a statistical approach, i.e., Vector Median Filters (VMF) [16], to a direct median extraction using a rank order filter (ROF). Ordering relations to be used to build the ROFs are **Esum**, **Lex**, **Marg**, and **CRA**. These ordering relations are selected since they consider a spectral image as a whole or, in other words, in a full-band way. And they are also the ones to be considered in Section IV, V, and VI.

A. Brief overview

Median filters belong to ROF family, thus requiring the use of an ordering relation. Mathematically, ROF can be expressed as in (14), where the notion of rank r is linked to cardinality c_v or the number of spectra that are 'smaller' than itself [12]. An ROF F of a defined filter window W, rank r, and ordering relation g takes a spectrum at the origin S_x as input and replaces it with a spectrum S_v that originates from W and

[1]Here, *accuracy* is used to be more easily understandable. Although in the metrological sense, it is *measurement error* that we are measuring, i.e., "the measured quantity value minus a reference quantity value" [24].

input values

A	B	A	C	A	B	E	D	F

ordered values

A	A	A	B	B	C	D	E	F

cardinality c_v

0	0	0	3	3	5	6	7	8

Fig. 2. A set of $n_W = 9$ letters as input values, to be ordered alphabetically. The mathematical expression in (14) allows to select a letter B (as marked in red) as the median of the set by means of its cardinality $c_v = 3 \le \frac{n_W - 1}{2}$.
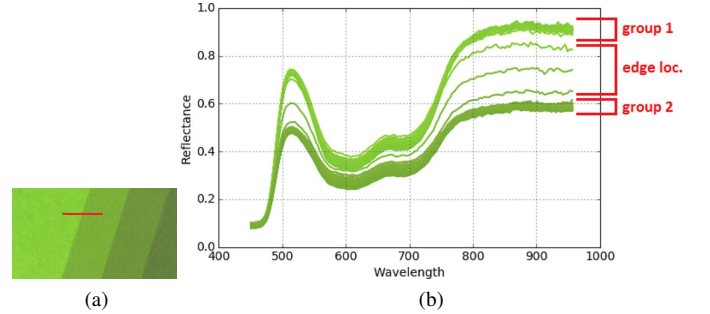
Fig. 3. Illustration of a pigment patch where **(a)** an arbitrary line segment shown in red line is chosen and **(b)** its spectra are plotted. Spectra belonging to the homogeneous green regions are grouped as *group 1* and *2*. Spectra of the edge pixels are shown in *edge loc.*. The pigment patch is of real pigment patch that was acquired by a hyperspectrally scanner.

whose cardinality is maximum among those with $c_v \le r - 1$. Then, two possibilities of input values may arise, i.e., all input values are unique or when identical values are present. When all values are unique, $c_v = r - 1$. To illustrate the latter, see Fig. 2. The occurrence of identical values obligates the constraint of $c_v \le r - 1$ to cater for the case when $c_v = r - 1$ does not exist.

$$F_{W,r,g}(x) = \bigvee \{S_v \mid c_v \le r - 1, \ S_v \in \mathscr{S}_W(x)\},$$
$$c_v = \#\{S_i \mid g(S_i) \le g(S_v), \ \forall S_i \in \mathscr{S}_W(x)\} \quad (14)$$

In an alternative approach, Astola [16] developed VMF under the definition of median as "the point of minimum aggregate distance or travel" [28], [5]. VMF obtains a median spectrum by extracting rank $r = 0$ using **Cumdist** in (10).

B. Assessment protocol of accuracy

Grayscale median filters are known for its edge preservation capability. To assess whether the spectral ones also has this property, accuracy assessment between the reference and filtered or obtained edges can be carried out. In this case, the reference edge will be obtained from the original image. Then, error assessment can be measured based on two criteria, i.e., sharpness and location of an edge. Pigment patches as in Fig. 3a will be employed for the experiment, where approximate locations of their edges are known. Then, instead of carrying out evaluation on an entire image, line segments $\mathscr{S}_L$ will be randomly selected from the image target as illustrated in Fig. 3a, where each is required to include two homogeneous regions. Spectra of pixels in the $\mathscr{S}_L$ are shown in Fig. 3b, where those belonging to the homogeneous regions (*group 1* and *2*) are highly similar in magnitude. As for spectra originating from the edge pixels (*edge loc.* group), magnitudes of their spectra are between the homogeneous groups.
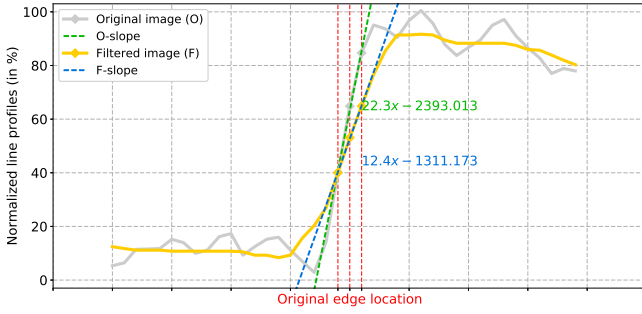
Fig. 4. An illustration of line profiles of an original image and its filtered image. Their edge slopes are approximated by polynomial functions of degree 1. A less steep slope indicates a blurrier image.

The determining element of a spectral median filter performance is a *line profile* ℓ. It is obtained by computing difference values of pixels in a line segment to a theoretical equi-energetic white spectrum $S_{wh} = \{s(\lambda) = 1, \forall \lambda \in [\lambda_{\min}, \lambda_{\max}]\}$, see (15). In this protocol, KLPD function [4] is chosen as the spectral difference function. From line profile ℓ, two objective criteria can be calculated, i.e., edge sharpness and location.

$$\ell = \{d(S_{wh}, S_i), \forall S_i \in \mathscr{S}_L\} \quad (15)$$

Let $y_o = a_o x + b_o$ and $y_f = a_f x + b_f$ be the linear approximations of edge slopes from an original and its filtered images, respectively, see illustration in Fig. 4. To quantify changes in edge sharpness after processing, (16) is used. $E_{sharp} \geq 1$ is considered to be good result, where the processed edge is either identical or sharper than the original. Blurred processed edge will yield value $0 < E_{sharp} < 1$. Zero and negative E_{sharp} correspond to when no edge is detected and when processed edge has different direction, respectively.

$$E_{sharp} = a_f/a_o \quad (16)$$

A well-performing median filter not only maintains the sharpness of an edge but also its location. Edge location shift will be quantified by (17), where score approaching 0 indicates better performance. To have statistical measures of mean μ and standard deviation σ, edge sharpness and location tests will be carried out $m = 500$ times, each time using a randomized pigment patch and line segment.

$$E_{shift} = | (-b_o/a_o) - (-b_f/a_f) | \quad (17)$$

Each pigment patch has different spectral distribution, causing the obtained line profiles to have varying dynamic ranges. To deal with this, normalization process in (18) will be applied to the line profiles (denoted ℓ_i for both original and filtered ones) obtained from the same line segment, relative to the VMF-generated one ℓ_{VMF}.

$$\bar{\ell}_i = 100\% \cdot \frac{\ell_i - \bigwedge \ell_{VMF} - \varepsilon}{\bigvee \ell_{VMF} - \bigwedge \ell_{VMF} + 2\varepsilon}, \quad (18)$$
$$\text{where } \varepsilon = k \cdot (\bigvee \ell_{VMF} - \bigwedge \ell_{VMF}), \ k = 0.1$$

TABLE II
AVERAGES μ AND STANDARD DEVIATIONS σ OF EDGE SHARPNESS E_{sharp} AND LOCATION SHIFT E_{shift} OBTAINED FROM 500 TESTS. BEST AND WORST RESULTS ARE COLORED GREEN AND RED, RESPECTIVELY.

Criteria		VMF (Cumdist)	Esum-MF	Lex-MF	Marg-MF	CRA-MF
E_{sharp}	μ	0.449	0.938	0.690	0.911	0.905
	σ	0.398	0.568	0.968	1.233	0.873
E_{shift}	μ	2.800	0.530	6.492×10^{14}	0.481	0.513
	σ	4.106	3.243	8.511×10^{15}	2.949	3.031
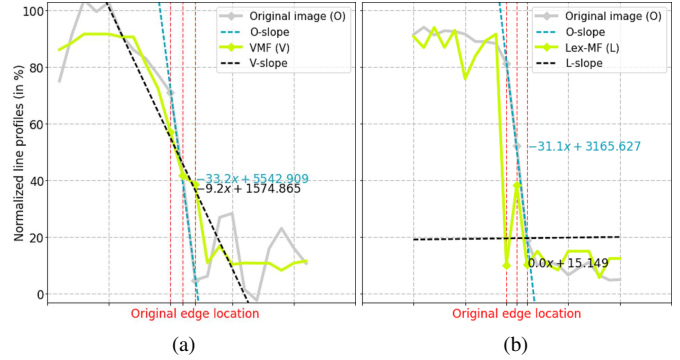
Fig. 5. Two examples of edge preservation cases given for **(a)** VMF and **(b)** Lex-MF. VMF and Lex-MF blurs and destroys the original input edges, respectively.

C. Performance assessment results

Results of edge sharpness and location shift tests are provided in Table II. There, it can be observed that the employed filters generally blur edges. The robust statistical approach of VMF is well reflected by the σ of E_{sharp}. However, looking at its μ, it becomes evident that VMF is the most blurring one. See also an example in Fig. 5a. And this is due to its assumption of symmetric exponential distribution [16] which is not satisfied by the employed dataset. Esum-MF is found to be the best performing median filter when it comes to maintaining edge sharpness E_{sharp}, providing μ that is closest to 1 compared to others. Its performance in maintaining the edge location is also relatively close to 0, especially when compared to VMF and Lex-MF.

Despite having a higher μ of E_{sharp} than the statistical VMF approach, Lex-MF demonstrates performance instability. And this behavior is especially reflected by its μ and σ of E_{shift} scores. An example problem encountered by Lex-MF is shown in Fig. 5b, where it essentially destroys the original input edge, yielding $a_f = 0$. In such a case, sharpness score $E_{sharp} = 0$ and $E_{shift} \to \infty$ will be obtained. In the sharpness test, this removal of edge indeed goes undetected due to formulation of the criteria and also the use of average measure. However, it will become evident in the edge location shift test. $a_f = 0$ can be interpreted as there being no edge or slope. But in order to avoid division by zero problem, in our implementation we chose to represent 0 by a very small number instead. Consequently, yielding a very big E_{shift}, that will be further propagated to the computation of μ and σ of E_{shift} values as observed in Table II. Note that these scores do not state that Lex-MF always perform bad, but rather of its unpredictability.

In terms of edge location preservation, in Table II, Marg-MF demonstrates the best performance among the rest. And this is as expected due to its independent processing for each spectral band, which can also be considered as a statistical one like VMF. At the same time, however, this independent band processing presents a drawback as captured by the σ of E_{sharp}. Shortly, it is because the mixing of information from independent spectral bands modifies spectral distribution in the line segment under consideration, hence a larger σ of E_{sharp}.

The last filter to assess is CRA-MF, which presents itself to be an alternative solution for spectral median filter. Considering both scores in edge sharpness test, its performance is only slightly below the best performing one, i.e., Esum-MF. Its μ of E_{sharp} is indeed lower than Marg-MF, but when its corresponding σ is also taken into account, CRA-MF can be concluded as more stable than Marg-MF. In edge location preservation test, CRA-MF places second after Marg-MF.

To summarize, performances of several spectral median filters have been assessed relative to a reference measure using two criteria, i.e., edge sharpness and location. 500 randomized tests were carried out and, from results in Table II, candidate solutions to spectral median filters are Esum-MF, CRA-MF, and Marg-MF. VMF is found to blur edges more than other filters, while Lex-MF demonstrates unstable performance.

IV. EFFICIENCY OF MEDIAN SPECTRUM EXTRACTION

In the context of image classification, the mean of all pixels is typically chosen as the representative pixel of a class. This can be found in, e.g., k-means clustering and machine learning methods such as self-organizing maps. Hyperspectral images are not vectors in the Euclidean space but should rather be considered as series or functions of wavelengths [4], [12]. Furthermore, the use of average computation erroneously assumes that there are valid addition and multiplication with a scalar in the spectral domain. As a consequence, representative pixels in the context of hyperspectral image classification should rather use an alternative way such as the median. In the following, efficiency of various ordering relations in extracting the median spectrum for each class in a hyperspectral image will be discussed and assessed. Performance in this test is correlated to the computational efficiency of ordering relations.

A. Computational complexity of spectral ordering relations

Due to the size of a hyperspectral image, computational complexity often becomes the main consideration when determining how they should be processed. In extracting a median spectrum from a set of spectra, the main task lies in sorting them. And here comes the role of an ordering relation. In addition to Esum, Lex, Marg, and CRA, the cumulative distance approach (Cumdist) will also be assessed. Their computational complexity are provided in Table III, where a median spectrum extraction task is broken down into three main tasks.

Pixel loading Due to the sheer size of a hyperspectral image, the simple task of reading and loading the pixels into memory has to be accounted for. And the cost for this task is linear following pixel and spectral band counts n and Λ, respectively.

Pre-sorting Depending on the ordering relation, certain processing will be required at this step. Cumdist requires to compute the distance between each pixel to every other pixels within the same class. This induces a quadratic complexity $n^2\Lambda^2$. This step is then followed by computing the cumulative distance for each pixel, costing $n\Lambda$. As for CRA, its distance map computation only requires linear time $n\Lambda$ since it only compute the distance of each pixel to two references. This step is then followed by the computation of ratio and angular maps of distance, which also takes a linear time. Esum requires to compute the sum of energy map, which takes a linear time $n\Lambda$.

Quicksort Assuming the use of quicksort, different ordering relations might need a different implementation. Cumdist and Esum can use the standard quicksort as they provide scalar values to the sorting algorithm, hence the quadratic n^2 cost. For Lex, quicksort is carried out sequentially across the spectral bands, inducing the standard cost multiplied by the number of spectral bands $n^2\Lambda$. CRA is also a conditional ordering relation like Lex. But since its condition is only 2, this multiplication factor can be considered negligible, yielding a complexity of n^2. Lastly, sorting complexity of Marg is $n^2\Lambda$ since quicksort is carried out independently for each spectral band.

Finally, from Table III, it can be concluded that the least efficient one is Cumdist. Then, the most efficient ones are Esum and CRA. In the following, these theoretical efficiencies will be assessed in a real experiment allowing to have a more complete knowledge.

B. Assessment protocol of efficiency

Efficiency assessment of an ordering relation will be carried out by simply calculating the time it requires to obtain median spectra of all classes in a given image. To conduct the experiment, three publicly available images will be employed, each comes with a ground truth information. Specifications of these images are provided in Table IV, where the total numbers of classes and pixels are excluding background information. Note that this experiment was developed using Python 2.7 and numpy 1.11.1 and was executed on a platform of Intel® Xeon® E3 processor, 8GB of RAM, and 64-bit Windows 7 operating system.

TABLE III
COMPUTATIONAL COMPLEXITY OF MEDIAN SPECTRUM EXTRACTION USING 5 SPECTRAL ORDERING RELATIONS. n AND Λ ARE NUMBERS OF PIXELS IN ANY ARBITRARY CLASS AND SPECTRAL BANDS IN THE IMAGE, RESPECTIVELY. GENERALLY, $\Lambda < n$.

Operations	Computation for each class in an image				
	Cumdist	Esum	Lex	Marg	CRA
Pixel loading	$n\Lambda$	$n\Lambda$	$n\Lambda$	$n\Lambda$	$n\Lambda$
Pre-sorting					
Distance map and	$(n\Lambda)^2$	-	-	-	$n\Lambda$
cumulative dist.	$n\Lambda$	-	-	-	-
CRA dist.	-	-	-	-	n
Sum of energy	-	$n\Lambda$	-	-	-
Quicksort*	n^2	n^2	$n^2\Lambda$	$n^2\Lambda$	n^2
Time complexity	$O(n^2\Lambda^2)$	$O(n^2)$	$O(n^2\Lambda)$	$O(n^2\Lambda)$	$O(n^2)$

TABLE IV
Specification of remote sensing images [29], [30] employed in the efficiency assessment of spectral ordering relations. Background class information is excluded from the table.

Images	Image size	Wavelength (in nm unit)	Numbers of	
			Classes	Pixels
Indian Pines	145×145×220	400 - 2500	16	10249
Pavia Univ.	610×340×103	400 - 2500	9	42776
Salinas	512×217×224	430 - 837	16	54129

TABLE V
Time required to compute median spectra of all class in an image, in unit of seconds. The least and most efficient ordering relations are Cumdist and Esum, respectively.

Image	Cumdist	Esum	Lex	Marg	CRA
Indian Pines	527.381	0.148	0.333	0.277	1.582
Pavia Univ.	9035.105	0.517	2.743	0.733	8.666
Salinas	13287.247	0.816	2.825	1.372	10.610

C. Performance assessment results

Efficiency of the 5 spectral ordering relations in a real case of median spectra extraction are provided in Table V. Esum is found to be the most efficient one, closely followed by Marg and Lex, which is unlike the theoretical efficiency drawn in Table III. This, however, is unsurprising. Even though theoretically Marg requires $n^2\Lambda$, its independent channel processing allows the implementation to be carried out as a matrix processing, making the factor Λ into a negligible constant. As for Lex, due its excessive prioritization of few first channels, the subsequent sorting process most likely does not have to visit all image channels. This can be seen by comparing the time it requires to process Indian Pines and Pavia Univ., compared to Marg ordering relation. In processing Indian Pines, the processing time is not significantly different from Marg, suggesting that perhaps only one or two channels were required to provide a decision. On the other hand, the difference of processing time between Marg and Lex for Pavia Univ. is larger, suggesting more image channels could be used by Lex to produce the median spectrum. CRA ordering relation, with identical theoretical efficiency to the Esum, is showing a lower performance than Esum by factors of 10 to 16. Finally, agreeing to results in Table III, the least efficient ordering relation is Cumdist. For Salinas image, Esum and CRA only requires 0.8 and 10.6 seconds, respectively. While for Cumdist, a total of approximately 3.7 hours are required to process the same image.

V. On the theoretical properties of morphological tools

Mathematical morphology (MM) provides the main framework for nonlinear image processing. It was originally developed for binary and grayscale images under metrological purposes, particularly for uses in granulometric measurements. There are several works extending this framework to the hyperspectral domain [20], [21]. However, they do not satisfy all theoretical requirements of the framework (Fig. 6). Due to this, stability of the results cannot be guaranteed. In other words, uncertainty of the results will not be stationary regardless of the spatio-chromatic complexity of the image content.
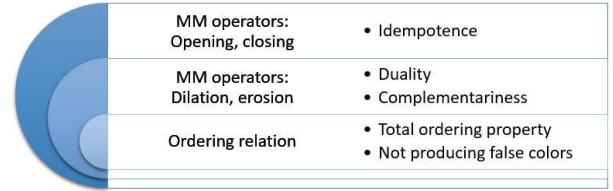
Fig. 6. Requirements or properties to be met in order to extend mathematical morphology framework to the multivariate domain.

(a)   (b)
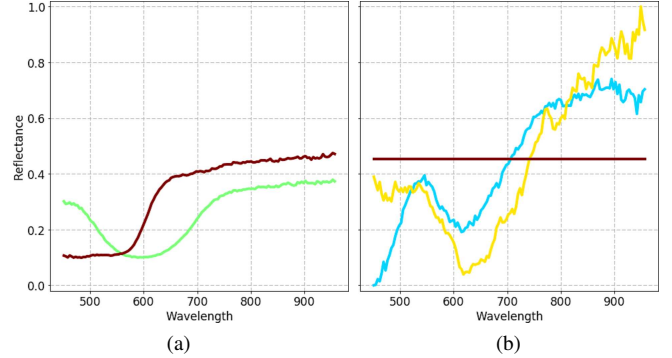
Fig. 7. Examples of cases causing **(a)** marginal and **(b)** sum of energy ordering relations to violate anti-symmetry property. In (a), marginal ordering relation is not able to determine which are the minimum and maximum. In (b), the three different spectra have the same amount of total energy, causing minimum/maximum spectrum indeterminable by sum of energy ordering relation.

A. Total ordering property

Metrology allows accessing the physical and optical properties of an analysed surface, since it treats images as physical measurements obtained from a light sensor, instead of mere mathematical objects. And to assess metrological properties, e.g., uncertainty and bias, only full-band MM approaches will be considered. At the core of MM, an ordering relation g is required to be "total" by respecting all properties below.

- Reflexivity, $S_1 \preceq_g S_1$.
- Transitivity, if $S_1 \preceq_g S_2$ and $S_2 \preceq_g S_3$ then $S_1 \preceq_g S_3$.
- Anti-symmetry, if $S_1 \preceq_g S_2$ and $S_2 \preceq_g S_1$ then $S_1 = S_2$.
- Trichotomy is where exactly one of the following holds: $S_1 \prec_g S_2$, $S_1 \succ_g S_2$, or $S_1 =_g S_2$ [31].

The most challenging property to satisfy is the anti-symmetry. It demands the uniqueness of the maximum or minimum of a set. When it is not satisfied, the expected metrological level of an MM cannot be reached because the results of MM becomes dependent on the uncertainty of minimum/maximum extraction. When this is the case, the MM operators are defined as pseudo-morphological operators [32], [33].

Lexicographic and other prioritization function-based ordering relations naturally reach anti-symmetry property because they code a multivariate data into a unique word. Marginal ordering relation do not satisfy this property since it cannot always order two multivariate data (Fig. 7a). For ordering based on sum of energy, different spectra can present the same energy level (Fig. 7b). And this problem is also suffered by ordering based on simple distance function. To address this limitation, Ledoux, et al. [15] proposed to combine 5 distances and also developed a theoretical study proving the validity of

its anti-symmetry property, ensuring total-order property for the color domain. Cumulative distance function cannot be used as ordering relation since it can only determine the median.

A direct extension of [15] to the spectral domain with n numbers of channels would require $n+2$ distances. But a mathematical conjecture was proposed [12], arguing that the probability of obtaining two spectra with identical distances to a 3rd reference is decreased together with the increase of spectral channel count. Thanks to this conjecture, CRA ordering relation which merges 2 ratios of 2 distances can reach anti-symmetry and, thus, defined as a total-order.

Considering the total-order property, prioritization function-based ordering relations can be deemed as better choices. However, if the physical sense of an ordering is taken into account, such orders are only mathematical constructions with inability to consider chromatic information. Moreover, convergences of the value space are implicitly defined towards equi-energetic black and white spectra. On the other hand, CRA allows selecting arbitrary spectra as the convergences, constraining them to be outside the convex-hull of the spectral set under evaluation [12].

B. On the notion of false spectra

False spectra are spectra generated after a processing, which do not exist in the initial spectral set. Among the 5 ordering relations that have been evaluated so far, the marginal one is creating this problem, unlike the rest which always pick a solution from within the initial set. Five spectra in Fig. 8a are given to marginal ordering in (2), their corresponding colors are also shown. Due to the channel-by-channel processing, the reflectance intensities are ordered independently of their initial spectra, causing the generation of 5 new ordered spectra in Fig. 8b. This problem is generally not perceptible due to integrations required in displaying in RGB spaces. Nevertheless, it induces a lack of accuracy in spectral processing.

C. Morphological properties

Having a valid ordering relation is not sufficient to ensure the validity of the morphological results. The validity of morphological results depends on the validity of erosion/ dilation operators, and then of the opening/ closing ones.

1) Duality and complementariness: Dilation and erosion are dual transformations with regards to complementation [31]. To achieve this, the complementary of relation g is defined by the difference to a maximum value M or by using an arithmetic inversion $-g$. Considering a spectrum as a set of measures and are therefore of positive values, the aforementioned duality approaches do not have any physical meaning, because there is no valid spectral addition and multiplication with a scalar.

In the context of prioritization function-based ordering relations, since no physical meaning is associated to them, the complementary operator can be defined by difference to maximum value M. For the marginal approach, complementariness is defined in the same manner, but independently for each channel. The CRA approach was carefully defined to account for physical senses of an ordering, using two spectral references and a spectral distance function. The references play
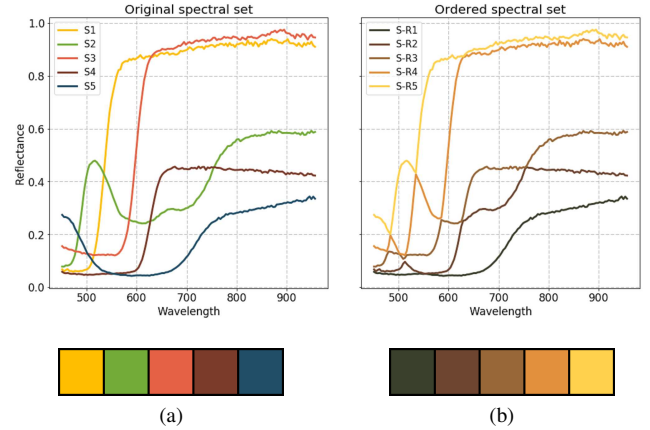
Fig. 8. Illustration of *false spectra* produced by marginal ordering relation. Given **(a)** an initial spectral set, marginal ordering relation orders the spectra independently in each spectral band, resulting in **(b)** a new set of spectra.

a role as in the natural extrema of scalar values $-\infty$ and $+\infty$. At the same time, these references provide a neutral coordinate in the middle on the segment they define. Consequently, a complementary spectrum is defined by means of symmetry to this neutral coordinate, allowing to develop the theoretical proof of CRA's duality.

2) Idempotency: Opening and closing transforms are required in order to construct more advanced morphological tools, e.g., granulometry and fractal signatures. As morphological filters, the following properties are required to ensure their validity: *translation-invariance*, *increasingness*, and *idempotency* [31]. While the first is related to the morphological construction, the last two are more about the ordering relation. Increasingness ensures that opening and closing preserve the ordering relations between images [31]. Idempotency ensures that multiple processing of opening Ψ (or closing Φ) will not modify results obtained after the first opening (or, respectively, closing), see (19).

$$\Psi \text{ is idempotent} \Leftrightarrow \Psi\Psi = \Psi \qquad (19)$$

In the context of marginal and prioritization ordering relations, idempotency and increasingness are naturally obtained. In the distance-based construction, an additional constraint must be enforced, linking dual operators for minimum and maximum extractions [34]. Typically, the minimum and maximum operators defined in [15] respect all expected properties of the first levels of morphological tools. However, they are not idempotent, i.e., the minimum expression is not exactly symmetrical to the maximum. Consequently, this approach introduces bias to opening and closing transforms, which will further impact the results. On the other hand, CRA ordering relation satisfies idempotency [12]. Its increasing property is easy to proof but is beyond the scope of this article.

VI. ACCURACY OF SPECTRAL BEUCHER'S GRADIENTS

The median filtering assessments in the previous sections address the question of spectral statistics close to the center of spectral distribution. On the other hand, morphological filters based on erosion and dilation allows assessing the maximum
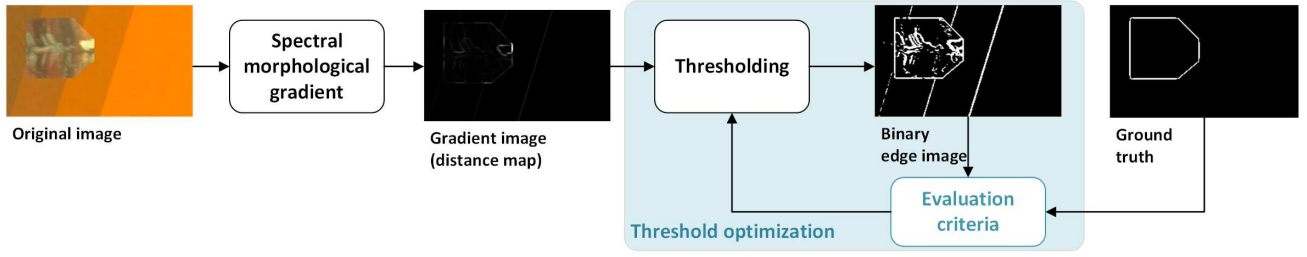
Fig. 9. Workflow of assessment protocol of gradient accuracy. Since the gradient operator produces a distance map, a thresholding process is required to produce a binary edge image. The best threshold for each distance map is obtained by maximizing evaluation criteria in (22).

and minimum. This further allows assessing the stability of ordering relation, especially since they are sensitive outliers [27], [35]. Thus, the next experiment will be based on the ability to extract gradient by means of the Beucher's gradient operator. Our hypothesis is that the gradient detection performance will decrease when the inner complexity of the proposed images increases. In parallel, performance differences between the ordering relations to test will be based on their robustness to the increasing inner complexity of the proposed images.

A. Brief overview

Image gradient captures directional changes of pixel values in the spatial coordinates of an input image. In this regard, it can be considered as an edge detector. And in the context of morphological image processing, image gradient is used as an intermediate processing tool. Its results are the prerequisite of image segmentation using watershed transformation.

In the grayscale domain, a Beucher's gradient operator is expressed as the dilation of a given image $\delta(I)$ subtracted by the eroded one $\varepsilon(I)$, see (20). Then, its extension to the spectral domain in (21) requires to replace pixel value difference by a valid spectral difference function, in which case is KLPD function [4].

$$\varphi(I) = \delta(I) - \varepsilon(I) \qquad (20)$$
$$= d(\delta(I), \varepsilon(I)) \qquad (21)$$

B. Assessment protocol of accuracy

Assessment protocol of accuracy is developed under the consideration of image gradient as an edge detector, employing pseudo-artificial images with known edge locations, see Fig. 9. To find the best threshold for each pair of input image and the employed gradient operator, threshold optimization is carried out by maximizing an evaluation criteria.

1) Dataset: Three datasets are employed where each comes with 112 images, i.e., KKA, KKB, and KFR datasets. Each image in the datasets is composed of background and foreground objects coming from hyperspectral acquisitions of pigment patches and a painting. Differences between the datasets lie in the complexity of chosen foreground objects. Background contents of KKA and KKB comes from pigment patches. Then, their foregrounds are showing a single and two homogeneous regions obtained from the patches, respectively. KFR is composed of background and foreground contents from pigment patches and a painting, respectively. See examples and their ground truth edge images in Fig. 10.
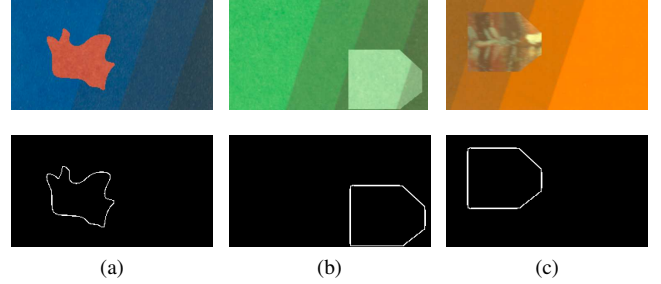
Fig. 10. Examples of image targets and their ground truth information from each dataset employed in the assessment of spectral Beucher's gradients, i.e., **(a)** KKA, **(b)** KKB, and **(c)** KFR. KKA and KKB have foreground objects which are of one and two homogeneous color regions, respectively. As for KFR, its foreground objects are extracted from a subset of a painting. All images are given in reflectance unit, from approximately 450 to 956 nm range.

2) Evaluation criteria: Each input image comes with a ground truth image showing the boundaries between background region and foreground object. Even though edges might also be present within background and foreground objects, in this assessment they will not be taken into account. With this, the evaluation criteria in (22) is employed; it was originally developed for edge map quality measure [36]. In this expression, n_f, n_O, n_{FP}, and n_{FN} are image target size, number of edge pixels in the ground truth edge image, number of false positive, and of false negative pixels in the edge image under evaluation, respectively. d_{FP_i} is distance between i-th false positive edge pixel and the nearest ideal edge pixel, d_{FN_i} is the distance between i-th false negative edge pixel and the nearest correctly detected edge pixel, and finally α is a penalty score set to $1/9$ as suggested by [37].

$$E = 1 - \frac{E_{FP} + E_{FN}}{2}, \text{ where}$$
$$E_{FP} = \frac{1}{n_f - n_O} \sum_{i=1}^{n_{FP}} \left(1 - \frac{1}{1 + \alpha d_{FP_i}^2}\right) \text{ and} \qquad (22)$$
$$E_{FN} = \frac{1}{n_O} \sum_{i=1}^{n_{FN}} \left(1 - \frac{1}{1 + \alpha d_{FN_i}^2}\right)$$

Values returned by (22) ranges from 0 to 1, where 1 signifies the highest accuracy score. To summarize the result for each dataset and employed ordering-based spectral Beucher's gradients, measures of average μ and standard deviation σ will be computed. With these measures, better performance is indicated by higher μ and at the same time lower σ.
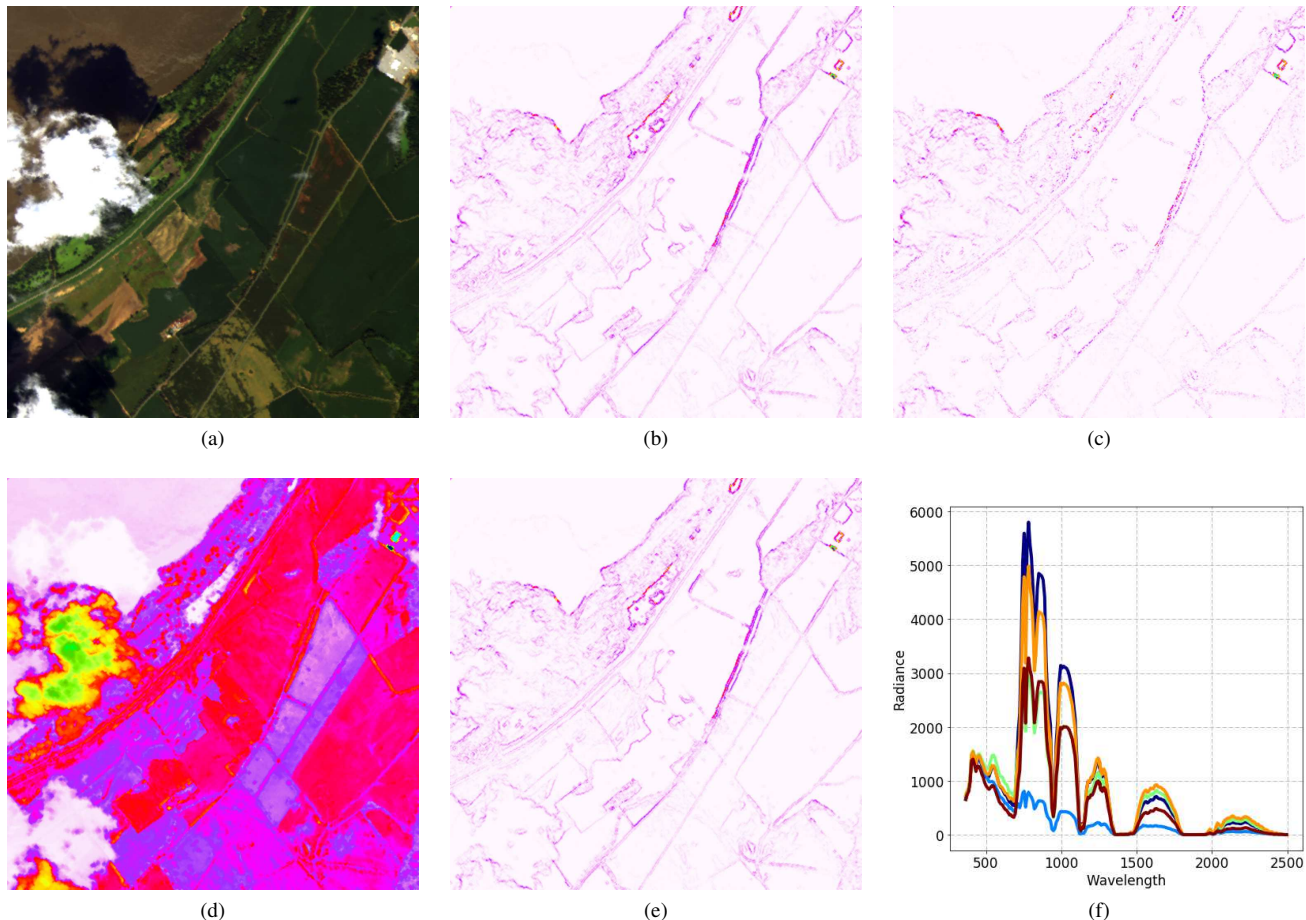
Fig. 11. **(a)** A 400×400 pixels subset of AVIRIS data as the original image and 4 of its gradient images as obtained by spectral morphological gradients based on the following ordering relations: **(b) Esum**, **(c) Lex**, **(d) Marg**, and **(e) CRA**. The gradient images are presented using a color map. **(f)** 5 radiance spectra randomly selected from the original image.

C. Performance assessment results

Assessment results of gradient accuracy using 3 pseudo-artificial datasets are summarized in Table VI. First of all, these measures are able to reflect the increasing content complexity from KKA, KKB, to KFR. μ and σ decreases and increases, respectively, almost in all of the employed ordering relations.

Results shown in Table VI suggest the superiority of marginal ordering relation. However, such results can be explained through the reduced spatio-chromatic complexity of the employed datasets. Background and foreground contents originating from pigment patches are relatively uniform and dominated by intensity variations. And this is why ordering relations such as the marginal, lexicographic, and Esum are able to solve the given tasks. However, using a real case such as a subset of AVIRIS data in Fig. 11, the limitations of Marg and Lex for morphological processing become evident. Marg ordering relation fails completely, while Lex returns broken or grainy gradients. In this figure, Esum and CRA show almost identical results. This is because more than 80% of spectra are located in the short-wave infrared range, where the spectral variations are reduced to mostly intensity variations, see Fig. 11f. To better highlight the limitation of Esum, an image with sufficient shape variations should be used.

TABLE VI
GRADIENT ACCURACY ASSESSMENT RESULTS OBTAINED FOR 3 DATASETS AND 4 SPECTRAL MORPHOLOGICAL GRADIENTS. PERFORMANCE SCORES RANGE FROM 0 TO 1 (SHOWN AS MULTIPLIED BY 10). HIGHER μ AND LOWER σ VALUES INDICATE BETTER PERFORMANCE.

Dataset	Esum		Lex		Marg		CRA	
	μ	σ	μ	σ	μ	σ	μ	σ
KKA	9.97	0.08	9.97	0.07	9.99	0.05	9.97	0.07
KKB	9.96	0.11	9.97	0.11	9.98	0.09	9.96	0.11
KFR	9.87	0.12	9.89	0.10	9.90	0.11	9.87	0.12

VII. DISCUSSION

In the previous sections, the behavior of spectral ordering relations have been analysed under several point of views, i.e., accuracy in the median filtering, computational efficiency of median value extraction, theoretical properties and physical sense of ordering relations, accuracy and usefulness in a low level image processing task using the Beucher's gradient expression. All of the obtained results are summarized in Table VII, providing readers with several elements of decision useful to select a suitable ordering relation for nonlinear hyperspectral image processing based on rank-order or MM approaches. In the quantitative tests, evaluated ordering relations are ranked from **1** (best) to **5** (worst). Regarding the qualitative properties

TABLE VII
SUMMARY OF COMPARISON BETWEEN ORDERING RELATIONS IN THE CONTEXT OF THEIR USES IN NON-LINEAR PROCESSING AND MATHEMATICAL
MORPHOLOGY (MM) FOR HYPERSPECTRAL IMAGES.

Criteria	Cumulative distance (Cumdist)	Sum of energy (Esum)	Lexicographic	Marginal	CRA
Accuracy (median filtering, section III)	5	1	4	2	3
Computational efficiency (median extraction, section IV)	5	1	3	2	4
Physical sense of the ordering (section V)	N.A.	N.A.	N.A.	N.A.	OK
Total order (MM, section V)	N.A.	N.A.	OK	N.A.	OK
Gradient detection (MM, section VI)	N.A.	3	3	1	2
Suitability for metrological use	N.A.	N.A.	N.A.	N.A.	OK

such as physical sense of ordering and total-order property, these ordering relations are given **OK** or **N.A.** if they satisfy or not the asked properties, respectively.

Cumdist is not a suitable approach for rank order or MM approaches. It only allows to extract median sample or spectrum using a statistical hypothesis based on distances. It does not include an ordering relation and, therefore, is not able to extract rank, minimum, or maximum that are required by the rank-order and MM processing. Furthermore, its use in the extraction of median spectrum becomes prohibitive since the computational cost is significant and there is no gain of accuracy when used in filtering [12].

Esum establishes rank based on the total energy of spectra under evaluation. This causes it to have no ability to account for chromatic information, since different spectra can have the same total energy. Due to this, it becomes difficult to analyse or understand the ranks it proposes, prohibiting to obtain total-order property. As shown in previous experiments, its results can be interesting for processing tasks such as median and gradient extractions using several datasets. It has to be kept in mind that, however, these results cannot be generalized to other datasets. Inability to satisfy total-order property means that robustness and stability of the process cannot be ensured.

Lex approach, and the similar bit-mixing one, are able to respect the total-order property. Constructed under mathematical coding point of view, they omit physical sense of data in their ordering processes. Due to this, small variations located in wavelengths that are given higher priority will significantly change the rank of the corresponding spectrum, causing incoherence between spectra with highly similar shape and/ or intensity. This lack of physical meaning in the ordering will have an impact in the management of local neighborhood in real images where spatio-chromatic complexity is high. In such cases, the small variations will induce processing bias, especially for use in texture assessment such as granulometry.

The **Marg** approach cannot produce total order and this problem becomes more critical as channel count increases. Due to inner construction of the data, few variations in spectral intensity at each wavelength can completely change the rank a spectrum is associated with. Finally, just as Esum, the seemingly relevant results of this approach is highly dependent on the nature of the used dataset. Its inability to comply to total-order constraint means that processing stability and quality cannot be guaranteed for all kinds of data.

The last ordering relation **CRA** did not obtain superior ranks in median filtering and gradient detection. It is, however, the only ordering relation that respects all of the other constraints. Indeed, the range of its physical understanding or interpretation are related to the spectral reference choice. However, for a more complete image processing analysis, it is possible to combine several references as shown in [4], [12]. Its compliance to total-order property is obtained due to a mathematical conjecture, which could be easily demonstrated in a future work. Finally, its ability to preserve the physical sense of data and order properties allows guaranteeing the result stability and robustness, regardless of the used datasets.

VIII. CONCLUSION

The increasing use of hyperspectral imaging for environmental, industrial, and cultural heritage purposes poses a high demand on the metrological processing of hyperspectral images. In this work, we have set the focus to the performance assessments of ordering-based nonlinear image processing approaches. Two groups of criteria have been defined. The first group includes quantitative evaluation of measurement errors and bias in the ordering process in, e.g., median filtering and gradient detection. The second group of criteria is based on compliance to expected theoretical properties and adherence to physical sense of data in the processing. Adherence to physical criteria of data ensures the metrological link between processing results and the optical or physical properties of materials or surfaces captured by the hyperspectral sensor.

Several evaluation results in this work have shown the necessity of identifying other spectral datasets for such performance evaluations. The lack of spatio-chromatic complexity of the dataset were unable to show the limitation of approaches that were deemed inappropriate by the theoretical requirements of an ordering relation. The simple datasets that were used have allowed these approaches to obtain good performance scores with respect to the proposed criteria. Nevertheless, from this work, it can be said that the CRA ordering approach is the first one to respect all expected constraints. It also presents good scores in the quantitative tests. Thus, CRA ordering relation can be used in metrological hyperspectral image processing and analysis.

In a future work, since performance scores of CRA in the quantitative tests were not the best ones among others, there is a place for identifying or defining better ordering relations. But it has to be remembered that the ordering relation must be defined in a "full-band" approach in order to preserve the physical nature of spectra, whether in radiance or reflectance.

IX. Acknowledgment

This work has been supported by French national projects ANR DigiPi and ERDF NUMERIC/ e-Patrimoine, and HyPerCept – Color and Quality in Higher Dimensions (Projectnr. 221073) funded by the Research Council of Norway. Authors would also like to thank the anonymous reviewers for providing invaluable feedback to this article.

References

[1] M. G. Kendall, "Discrimination and classification," in *Multivariate analysis*. Academic Press, 1966, pp. 165–185.

[2] C. B. Bell and H. S. Haller, "Bivariate symmetry tests: Parametric and nonparametric," *Ann. Math. Stat.*, vol. 40, no. 1, pp. 259–269, 1969.

[3] H. Deborah, N. Richard, and J. Y. Hardeberg, "A comprehensive evaluation on spectral distance functions and metrics for hyperspectral image processing," *IEEE J. Sel. Topics Appl. Earth Observ. Remote Sens.*, vol. 8, no. 6, pp. 3224–3234, 2015.

[4] N. Richard, D. Helbert, C. Olivier, and M. Tamisier, "Pseudo-divergence and bidimensional histogram of spectral differences for hyperspectral image processing," *J. Imaging Sci. Technol.*, vol. 60, no. 5, pp. 1–13, 2016.

[5] V. Barnett, "The ordering of multivariate data," *J. R. Stat. Soc. Ser. A*, vol. 139, no. 3, pp. 318–355, 1976.

[6] E. Aptoula and S. Lefèvre, "A comparative study on multivariate mathematical morphology," *Pattern Recognition*, vol. 40, no. 11, pp. 2914–2929, 2007.

[7] E. Aptoula, S. Lefèvre, and C. Collet, "Mathematical morphology applied to the segmentation and classification of galaxies in multispectral images," in *14th European Signal Processing Conference*, 2006.

[8] H. Deborah, N. Richard, and J. Y. Hardeberg, "Spectral ordering assessment using spectral median filters," in *Mathematical Morphology and Its Applications to Signal and Image Processing*. Springer International Publishing, 2015, pp. 387–397.

[9] I. Baghli and A. Nakib, *Lexicographic Approach Based on Evidence Theory for Blood Cell Image Segmentation*. Springer Berlin Heidelberg, 2017, pp. 137–154.

[10] M. A. Veganzones and M. Graña, "Lattice auto-associative memories induced supervised ordering defining a multivariate morphology on hyperspectral data," in *Hyperspectral Image and Signal Process.: Evolution in Remote Sens. (WHISPERS), 3rd Workshop on*, 2012, pp. 1–4.

[11] S. Velasco-Forero and J. Angulo, "Supervised ordering in $\mathbb{R}^p$: Application to morphological processing of hyperspectral images," *IEEE Trans. Image Process.*, vol. 20, no. 11, pp. 3301–3308, 2011.

[12] H. Deborah, "Towards spectral mathematical morphology," phdthesis, Norwegian University of Science & Technology, University of Poitiers, Dec. 2016. [Online]. Available: http://goo.gl/AsfCjj

[13] J. Chanussot and P. Lambert, "Bit mixing paradigm for multivalued morphological filters," in *Image Processing and Its Applications, 6th International Conference on*, vol. 2, 1997, pp. 804–808.

[14] D.-H. Wang, X.-K. Yang, and Y. Zhao, "A hyperspectral image endmember extraction algorithm based on generalized morphology," *Optoelectronics Letters*, vol. 10, no. 5, pp. 387–390, 2014.

[15] A. Ledoux, N. Richard, A.-S. Capelle-Laizé, and C. Fernandez-Maloigne, "Perceptual color hit-or-miss transform: application to dermatological image processing," *Signal, Image and Video Processing*, pp. 1–11, 2013.

[16] J. Astola, P. Haavisto, and Y. Neuvo, "Vector median filters," *Proc. IEEE*, vol. 78, no. 4, pp. 678–689, 1990.

[17] A. Plaza, P. Martinez, J. Plaza, and R. Perez, "Dimensionality reduction and classification of hyperspectral image data using sequences of extended morphological transformations," *IEEE Trans. Geosci. Remote Sens.*, vol. 43, no. 3, pp. 466–479, 2005.

[18] S. Velasco-Forero and J. Angulo, "Multiclass ordering for filtering and classification of hyperspectral images," in *Hyperspectral Image and Signal Process.: Evolution in Remote Sens. (WHISPERS), 3rd Workshop on*, 2011, pp. 1–4.

[19] N. Courty, E. Aptoula, and S. Lefèvre, "A classwise supervised ordering approach for morphology based hyperspectral image classification," in *Pattern Recognition (ICPR), 21st Intl. Conf. on*, 2012, pp. 1997–2000.

[20] E. Aptoula, N. Courty, and S. Lefèvre, "An end-member based ordering relation for the morphological description of hyperspectral images," in *IEEE Intl. Conf. on Image Processing (ICIP)*, 2014, pp. 5097–5101.

[21] N. Falco, J. A. Benediktsson, and L. Bruzzone, "Spectral and spatial classification of hyperspectral images based on ica and reduced morphological attribute profiles," *IEEE Trans. Geosci. Remote Sens.*, vol. 53, no. 11, pp. 6223–6240, 2015.

[22] J. Liang, J. Zhou, and Y. Gao, "Tensor morphological profile for hyperspectral image classification," in *IEEE Intl. Conf. on Image Processing (ICIP)*, 2016, pp. 2197–2201.

[23] X. Huang, W. Yuan, J. Li, and L. Zhang, "A new building extraction postprocessing framework for high-spatial-resolution remote-sensing imagery," *IEEE J. Sel. Topics Appl. Earth Observ. Remote Sens.*, vol. 10, no. 2, pp. 654–668, 2017.

[24] "Intl. vocabulary of metrology – Basic and general concepts and associated terms," http://goo.gl/AJIIoz, JCGM, Tech. Rep., 2012.

[25] P. Maragos and R. Schafer, "Morphological filters–part I: Their set-theoretic analysis and relations to linear shift-invariant filters," *IEEE Trans. Acoust., Speech, Signal Process.*, vol. 35, no. 8, pp. 1153–1169, 1987.

[26] ——, "Morphological filters–part II: Their relations to median, order-statistic, and stack filters," *IEEE Trans. Acoust., Speech, Signal Process.*, vol. 35, no. 8, pp. 1170–1184, 1987.

[27] I. Pitas and A. N. Venetsanopoulos, "Nonlinear or statistic filters for image filtering and edge detection," *Signal Processing*, vol. 10, no. 4, pp. 395–413, 1986.

[28] T. L. Austin Jr., "An approximation to the point of minimum aggregate distance," *Metron*, vol. 19, pp. 10–21, 1959.

[29] M. F. Baumgardner, L. L. Biehl, and D. A. Landgrebe, "220 band AVIRIS hyperspectral image data set: June 12, 1992 Indian Pine test site 3," http://purr.purdue.edu/publications/1947/1, Sep. 2015.

[30] M. A. V. Bodón, I. Marqués, and B. A. Vilches, "Hyperspectral remote sensing scenes," http://goo.gl/aDI8SW, Apr. 2014.

[31] P. Soille, *Morphological Image Analysis: Principles and Applications*, 2nd ed. Springer-Verlag New York, Inc., 2003.

[32] J. Larrey-Ruiz, R. Verdú-Monedero, J. Morales-Sánchez, and J. Angulo, *Towards Morphological Image Regularization Using the Counter-Harmonic Mean*. Springer Berlin Heidelberg, 2013, pp. 317–328.

[33] A. Căliman, M. Ivanovici, and N. Richard, "Probabilistic pseudo-morphology for grayscale and color images," *Pattern Recognition*, vol. 47, no. 2, pp. 721–735, 2014.

[34] R. Goutali, N. Richard, A. Ledoux, and N. Ellouze, "Problématique de l'idempotence pour les images couleurs et multivaluées," *Traitement du Signal*, vol. 31, no. 3-4, pp. 293–305, 2014.

[35] R. Lukac, B. Smolka, K. N. Plataniotis, and A. N. Venetsanopoulos, "Vector sigma filters for noise detection and removal in color images," *J. Vis. Commun. Image Represent.*, vol. 17, pp. 1–26, 2006.

[36] K. Panetta, C. Gao, S. Agaian, and S. Nercessian, "A new reference-based edge map quality measure," *IEEE Trans. Syst., Man, Cybern., Syst.*, vol. 46, no. 11, pp. 1505–1517, 2016.

[37] Q. Zhu, "Efficient evaluations of edge connectivity and width uniformity," *Image & Vision Computing*, vol. 14, no. 1, pp. 21–34, 1996.

Hilda Deborah received her PhD in 2016 from a co-tutelle arrangement between NTNU - The Norwegian University of Science and Technology and the University of Poitiers in France. Prior to that, she obtained her MSc degree from Erasmus Mundus Color in Informatics and Media Technology (CIMET) in 2013 and BSc in Computer Science from the University of Indonesia in 2010. She is currently a postdoctoral researcher at the Department of Computer Science at NTNU and a member of the Norwegian Colour and Visual Computing Laboratory. Her current research interests and activities lie in the more fundamental development of hyperspectral image processing framework, metrological assessment protocols for the said framework, as well as applications in the cultural heritage and remote sensing fields.

Noël Richard received his MSc and PhD degrees from the University of Poitiers in 1988 and 1993, respectively. He is currently Associate Professor at the University of Poitiers and researcher at XLIM laboratory, UMR CNRS 7552 since 1992, where has been working on color image processing for more than 20 years. He is the technical chair of the CIE Technical Committee TC8.14, working on the definition and assessment of spatio-chromatic complexity. Facing the lack of stability and accuracy of the existing approaches in color image processing, he developed a new image processing paradigm based on distance functions and non-linear expressions for metrological purposes. Since 2013, he has been extending the paradigm to hyperspectral images, where a full-band vector processing is developed to respect the metrological constraints.

Jon Yngve Hardeberg received his sivilingeniør (MSc) degree in signal processing from the Norwegian Institute of Technology in Trondheim, Norway in 1995, and his PhD from Ecole Nationale Supérieure des Télécommunications in Paris, France in 1999. After a short but extremely valuable industry career, he returned to academia and Norway in 2001. He is currently Professor of Colour Imaging at the Department of Computer Science at NTNU. He is a member of the Norwegian Colour and Visual Computing Laboratory, where he teaches, supervises MSc and PhD students, manages international study programs and research projects, and conducts research. His current research interests include multispectral colour imaging, print and image quality, colorimetric device characterisation, appearance, medical imaging, and cultural heritage imaging, and he has co-authored more than 200 publications within the field.

Christine Fernandez-Maloigne is currently the vice-rector in charge of International Relations at the University of Poitiers and director of CNRS research federation (MIRES), which gathers 560 researchers in the south west of France, in the area of mathematics, image processing, computer graphics, computer science, and communication systems. She is also an appointed member of the National Council of the French Universities (CNU), secretary of Division 8: Image Technologies of the CIE (International Commission on Illumination), and deputy editor-in-chief of JOSA A. Her research activities are focused on color imaging, including the fundamental research of the introduction of human visual system models in multiscale color image processing, as well as practical applications for biomedical, cultural heritage, and audio-visual digital contents.